AUT Journal of Electrical Engineering

AUT J. Elec. Eng., 55(2) (2023) 133-144
DOI: 10.22060/eej.2023.21972.5501

Proposing a THz refractive index sensor based on the excitation of SPPs with an InSb cylinder

S. Zamani Noughabi[1], A. S. Nooramin[2]*, M. Soleimani[3]

Department of Electrical Engineering, The Iran University of Science and Technology (IUST), Tehran. Iran

ABSTRACT: A novel metamaterial absorber sensor has been proposed for refractive index measurement in the range of [1-2] for the THz frequency band. This structure is based on using a plasmonic coaxial resonator which is excited by an InSb cylinder. Surface Plasmon Polaritons (SPPs) are excited on the surface of the InSb cylinder due to an inward plane wave and propagate downward toward the cavity and through it. Based on the radius and height of the InSb cylinder, the "high-absorption" and "high-quality factor" sensing performance is introduced and analyzed. It is shown that nearly 98% absorption can be achieved for all the range of refractive index [1-2] at 1.8622 THz and in the case of "high-quality factor", absorption reaches nearly 100% for the refractive index range of [1.5-2]. Also, by changing the radius and height of the cavity, absorption can be changed. Furthermore, sensitivity, quality factor, and figure of merit in the range of 166-672 GHz per refractive index unit (GHz/RIU), 69.1-118.7 and 10.2-29.7 is achievable, respectively. A wide range of refractive index measurements besides superior sensing performance made this structure a good candidate for sensing applications such as medical and biological applications.

Review History:

Received: Nov. 28, 2022
Revised: Jan. 08, 2023
Accepted: Feb. 21, 2023
Available Online: Oct. 01, 2023

Keywords:

Absorber metamaterial
coaxial plasmonic resonator
InSb
surface plasmons

1- Introduction

Metamaterial absorbers based on Surface PlasmonPolaritons (SPPs) have found many applications in narrow-band refractive index sensing applications[1]. These structures are usually comprised of metal-dielectric periodic structures in the sub-wavelength dimensions[2]. Metals, InSb, have been utilized for the excitation of SPPs which usually leads to an enhancement of the quality factor of the structure[3, 4]

The sensing performance of sensors can be evaluated by sensitivity (*S*) and Figure of Merit (*FoM*) which are defined as $S = \Delta\lambda/\Delta n$ and $FoM = S/FWHM$ [4], respectively. $\Delta\lambda$ is the shift of resonance frequency induced by changes in refractive index Δn. The *FWHM* is the full width at half maximum of the absorption spectrum.

To date, many plasmonic metamaterial absorbers have been proposed for sensing applications[3]. In[5], a metamaterial absorber sensor has been proposed for a range of refractive index[2, 3], quality factor, S, and FoM of 126, 44, and 10.5, respectively. Furthermore, S and FoM equal to 96.2 and 7.8, respectively are achieved for the measurement range of refractive index [1-2.5] by a metamaterial sensor[6]. It should be noted that the refractive index of analytes in biomedical applications such as cancer cell detection, blood sugar measurement, … are generally reported in the range of [1-2][2, 7] Therefore, the focus of this article is to propose a sensor for the measurement of the refractive index in mentioned range.

In this paper, we proposed a refractive index sensor based on the plasmonic coaxial metamaterial absorbers. Simulation results show that the sensitivity, quality factor, and *FoM* in the range of 166-672 GHz per refractive index unit (GHz/RIU), 69.1-118.7 and 10.2-29.7 have been achieved, respectively. Furthermore, we investigate the sensing performance of the structure by scanning the structural parameters of the structure and introducing "high-absorption" and "high-quality factor" sensing performances.

This paper consists of three sections. The design and simulation of the structure are explained in section 2. The analysis of sensing performance is represented in section 3. Finally, some conclusions are remarked in section 4.

2- Design and simulation of the structure

As shown in Fig. 1(a), the unit cell of the proposed structure is comprised of a thin layer of topas [8] which is covered by two golden sheets, in which a cylindrical tubular cavity has been extracted from the upper golden layer. This cavity has been excited by an incident THz plane wave while the resonance frequency is dependent on the filled analyte in the cavity. Therefore, the refractive index measurement of the analyte can be attained. The geometrical parameters and their values are presented in Table 1.

*Corresponding author's email: A_nooramin@iust.ac.ir

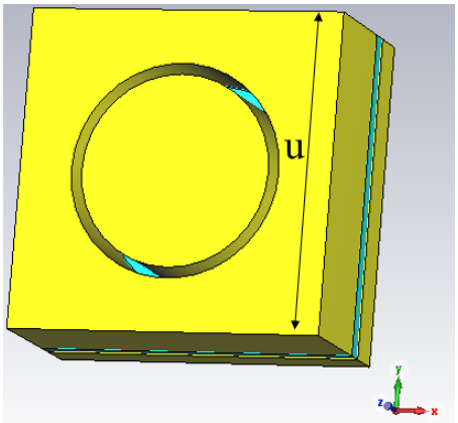

(a)

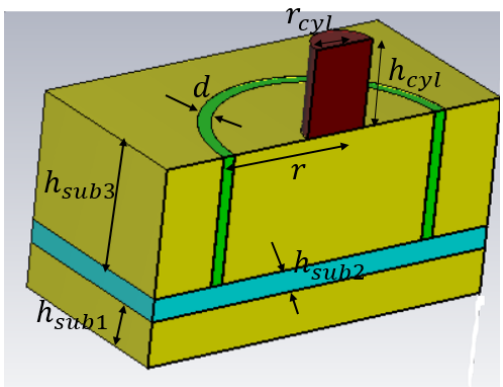

(b)

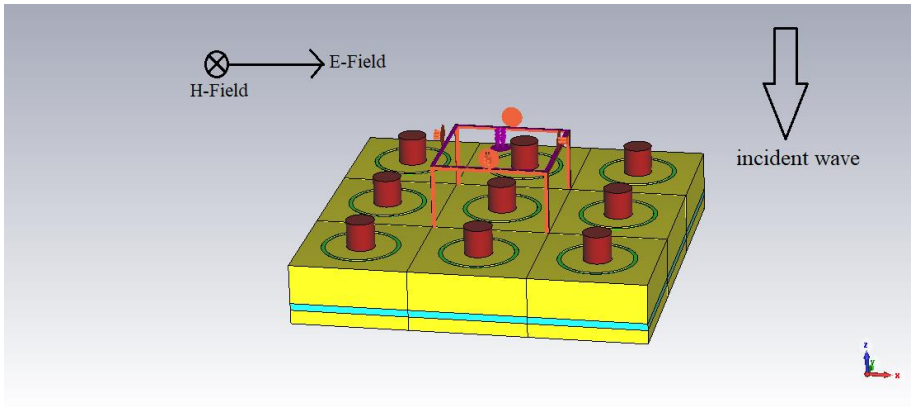

(c)

Fig. 1. Unit cell of structure (a) top view of basic structure. (b) Cutaway side view. (c) the periodicity of the structure and the direction of an incident plane wave.

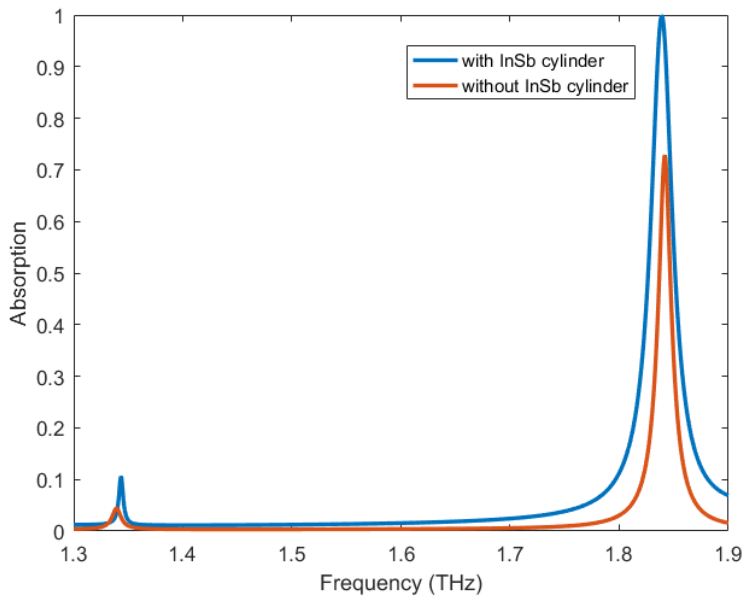

Fig. 2. Absorption graph with and without InSb cylinder.

The analysis in this paper has been done using CST software. As shown in Fig. 1(c), periodicity in the x and y directions of the structure is modeled by periodic boundary conditions, and an incident plane wave opposite the z-direction has been attained using the Flouqet port. In this simulation, S-parameters are calculated and values proportional to the absorption are derived from the following equation:

$$A = 1 - T - R = 1 - |S_{21}|^2 - |S_{11}|^2 \tag{1}$$

Where T and R stand for reflected and transmitted power. Since a relatively thick golden sheet is placed in the bottom layer of the structure, the value of T is assumed to be zero.

The absorption spectrum for the proposed structure is plotted in Fig. 2. As shown in this Fig, a narrow absorption spectrum is achieved whereas the maximum value of absorption is 0.7.

To improve the peak of the absorption spectrum and sensing performance as a result, a cylinder of InSb is placed coaxially and on top of the tubular cavity, as shown in Fig. 1(b). In this structure, surface plasmon polaritons (SPPs) are excited by an incident plane wave. Therefore, an enhancement in the peak of the absorption spectrum can be expected. To examine this, a drude model is assumed for InSb according to[9],

$$\varepsilon(\omega) = \varepsilon_\infty - \frac{\omega_p^2}{\omega^2 + i\omega\gamma} \tag{2}$$

Here, ε_∞ , ω_p , ω , and γ are stands for high-frequency dielectric constant, plasma frequency, angular frequency, and damping constant, respectively. The values of these parameters are shown in Table 1, according to[3]. An enhancement in the peak of absorption can be shown in Fig. 2.

To evaluate the improvement in the absorption ratio, the plasmonic mode of the structure has been studied more precisely. In Fig. 3(a) and Fig. 3(b), the plasmonic modes of the InSb waveguide and coaxial waveguides which can be excited by the plane wave are shown, respectively. As shown in this figure, the electric field distribution of these modes is the same, relatively. Furthermore, the wave impedance of these modes is plotted versus frequency in Fig. 4. As shown in this figure for 1.862 THz, the impedance of InSb and coaxial waveguide are 369.1 Ohm and 429.4 Ohm, respectively. Because the impedance value of the InSb waveguide is close to the impedance of air, it can be expected that this waveguide is better excited by the plane wave radiation. Due to the similarity of the spatial distribution of the electric fields of these two waveguides, the excitation of the coaxial waveguide will be done well by the InSb waveguide.

The peak value of absorption at the resonance frequency and the quality factor are analyzed as a function of the radius and height of the InSb cylinder, as shown in Fig. 5 and Fig. 6.

The values of absorption at resonance frequency depend on the height and radius of the structure, and its maximum value is attained for $r_{cyl} = 18$ µm and $h_{cyl} = 35$ µm, as obvious in

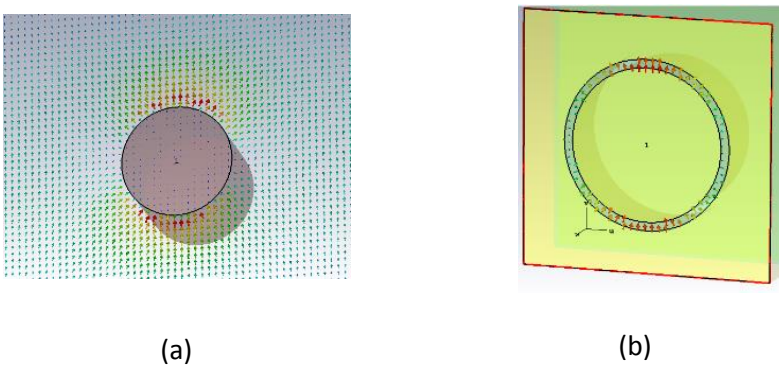

Fig. 3.The plasmonic mode of (a) InSb waveguide and (b) coaxial waveguide which can be excited by the plane wave radiation

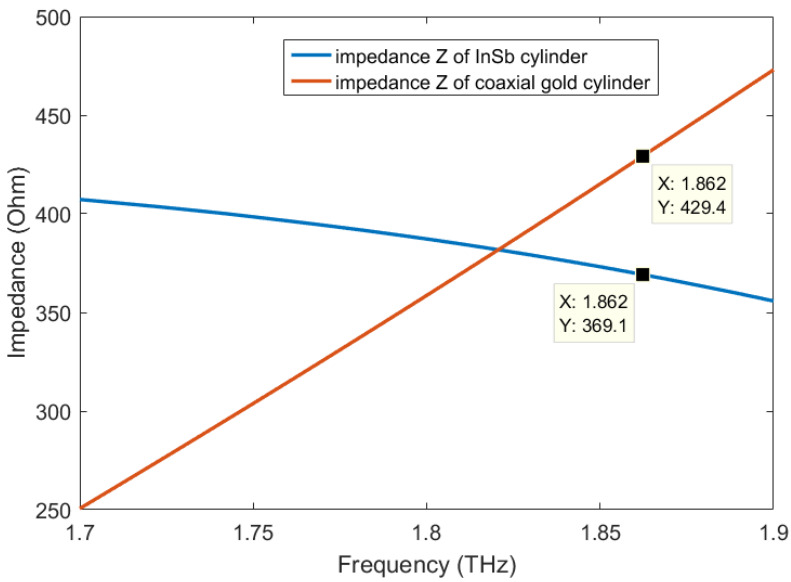

Fig. 4. The wave Impedance of InSb cylindrical waveguide and golden coaxial waveguide

Table 1. Value and unit of the parameter structure.

Parameter	Value	Unit
u	150	µm
r	50	µm
d	5	µm
h_{sub1}	18	µm
h_{sub2}	9	µm
h_{sub3}	51	µm
σ_{gold}	4.561e+7	S/m
ε_{sub2}	2.2	F/m
ε_{∞}	15.6	F/m
ω_P	65094527713652	rad/s
γ	0.31415e+12	1/s

S/m= siemens per meter , F/m= farad per meter , rad/s= radian per second.

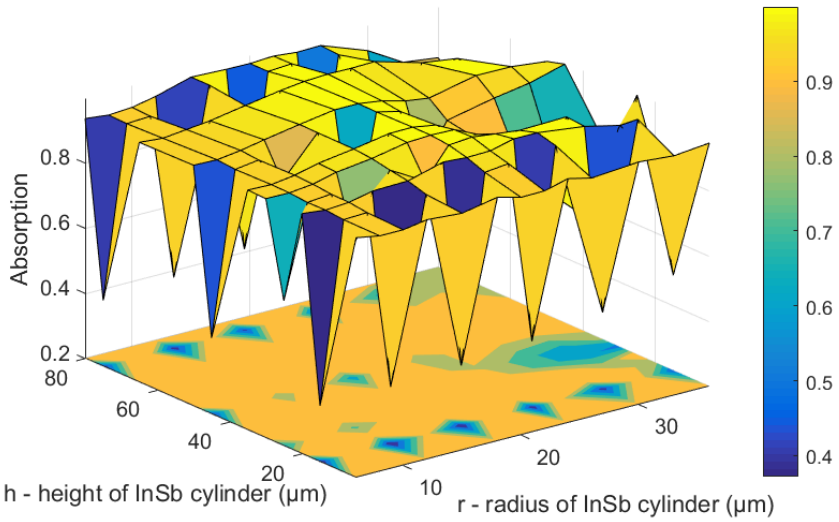

Fig. 5. Absorption graph with the change of radius and height of InSb cylinder.

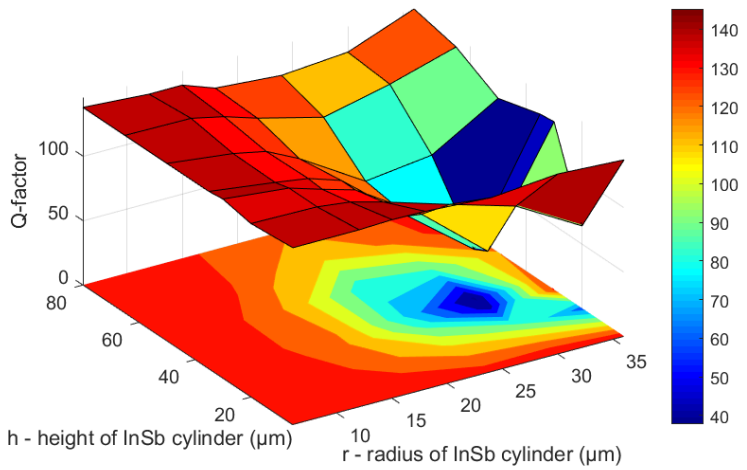

Fig. 6. Q-factor of the proposed sensor for different values of radius and height of InSb cylinder.

Fig. 5. Furthermore, the evaluation of the dependence of the quality factor on the radius and height of the InSb cylinder shows that its maximum value is obtained for $r_{cyl} =$ 36 μm and $h_{cyl} = 80$ μm.

Therefore, based on the selected values of r_{cyl} and h_{cyl}, high absorption or high-quality factor performance of sensing can be attained. These sensing performances will be examined in more detail below. It is worth mentioning that the above analysis is done based on the assumption of $n = 1.1$.

The absorption spectrum for refractive index values in the range of [1-2] is obtained and plotted in Fig. 7. Nearly 100% absorption is achieved for a high absorption performance sensor, as shown in Fig. 7(a). In the same way, a nearly unit absorption is obtained for values of the refractive index in the range of [1.5-2] and its value decreases to 0.6 for $n = 1$, as shown in Fig. 7(b). Furthermore, it can be realized that the values of the resonance frequency of the sensor in two cases of high absorption and high-quality factor sensing performance are the same as shown in Fig. 8. Further sensing performance of the sensor will be analyzed in the next section.

3- Analysis of the sensing performance of the structure

Three basic parameters are defined for the characterization of the sensing performance of sensors. The first one, the quality factor which describes the frequency-selecting ability of the sensor is studied and represented in Fig. 9(a). As shown in this figure, higher-quality factors are attained in nearly all the refractive indices [1-2] for the selection of high-quality factor sensing performance. Since the absorption spectrum in high absorption sensing performance remains constant for the refractive index in the range of [1-2], it is expected that a relatively constant quality factor is also attained, as shown in Fig. 9(a). Similarly, due to the reduction of the absorption peak by increasing the refractive index of high-quality factor sensing performance, the quality factor is expected to decrease, which is evident in Fig. 9(a). Hence, the Sensitivity (*S*) for both sensing performances is relatively the same, as shown in Fig. 9(b). In fact, sensitivity represents the response level of the sensor to the external factors to be measured. Furthermore, the Figure of Merit (*FoM*) for both sensing performances is also relatively the same, as shown in Fig. 9(c). *FoM* is defined as the ratio between the sensitivity and the full width at half maximum (*FWHM*) of the absorption peak and is a comprehensive parameter to evaluate the performance of an absorptive sensor[7].

In Fig. 10, the absorption diagram for $n =$ 1.1 for different values of height and radii of the analyte is drawn. As it is known, the best values to achieve maximum absorption can be attained from this figure.

The absorption spectrum for $n = 1.1$ is examined for different values of the polarization angle of an incoming plane wave, as plotted in Fig. 11. Since the structure is symmetrical, a polarization-insensitive nature is expected, as shown in Fig. 11.

The performance comparison of the proposed structure with previous works is given in Table 2. As can be seen in this table, higher quality factor, Sensitivity, and *FoM* in a wider range of refractive indices are attained.

The distribution of exciting electric fields in the structure by the incoming plane wave is given in Fig. 12. As shown in this Fig, SPPs are excited on the top surface of the InSb cylinder (Fig. 12(a)). Then, it propagates downward from the perimeter of the structure (Fig. 12(b)), and the electric fields of the cylindrical cavity will be excited (Fig. 12(c)), and propagate down the cavity (Fig. 12(d)) .Finally, the electric fields enter the topas layer and propagate toward the axis of the structure (Fig. 12(e)). It is worth mentioning that this simulation is done for $n = 1$ and $f = 1.8622$ THz.

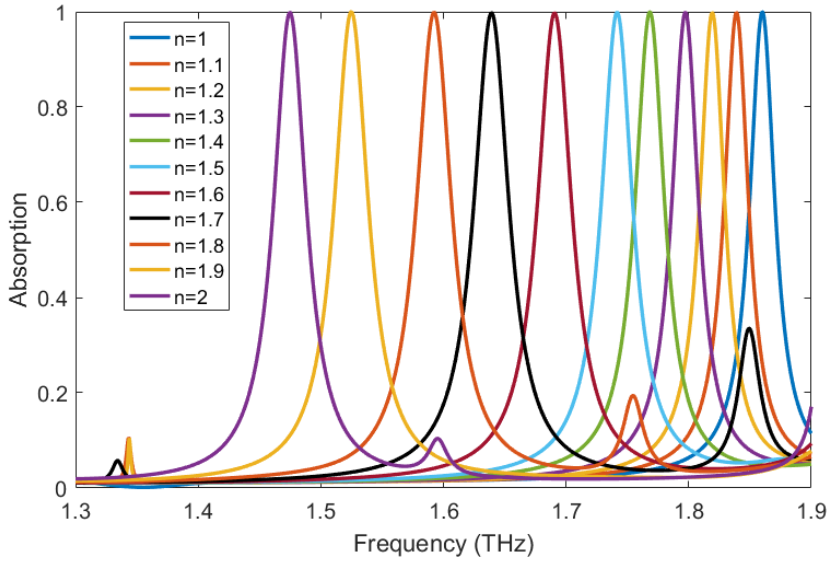

(a)

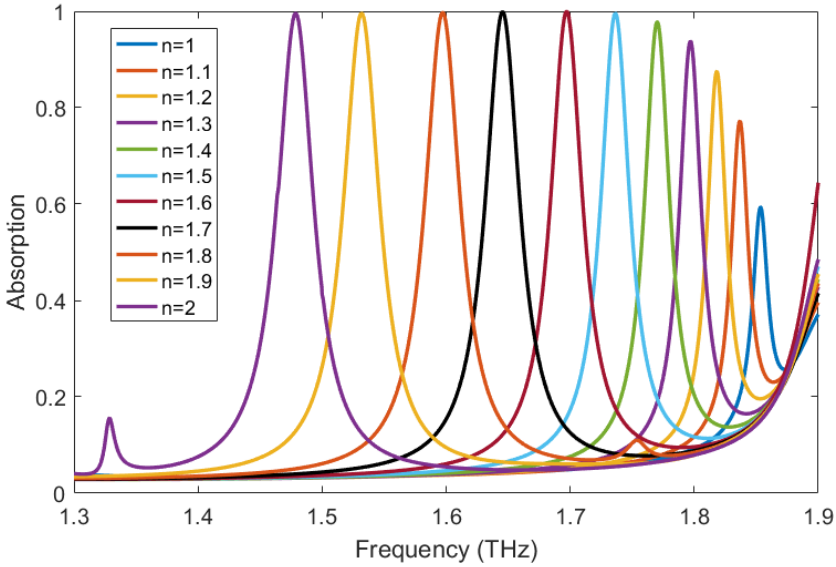

(b)

Fig. 7. Absorption graph for various refractive indices of the analyte. (a) high absorption and (b) high-quality factor sensing operation.

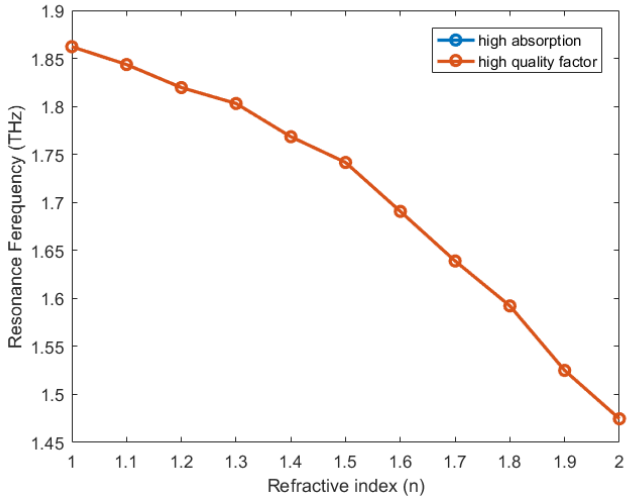

Fig. 8. Resonance frequency versus refractive index for two choices of high absorption and high-quality factor.

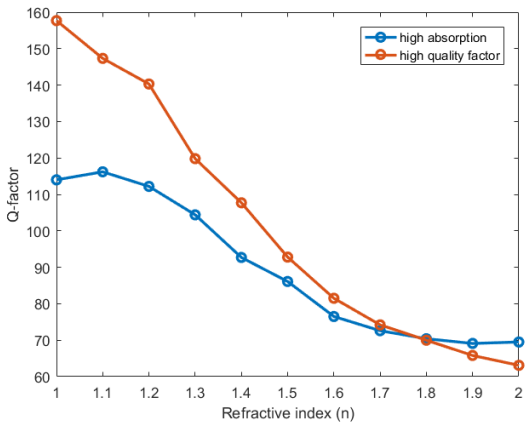

(a)

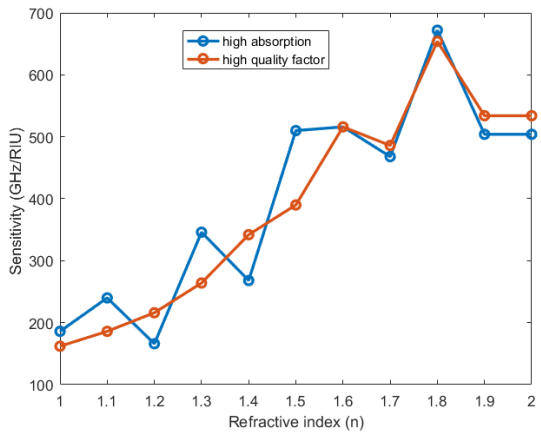

(b)

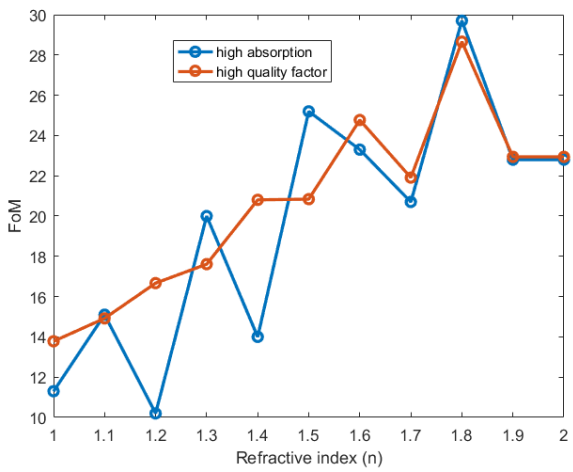

(c)

Fig. 9. (a) sensitivity, (b) FoM, and (c) Q-factor for two choices of "high absorption" and high-quality factor" sensing performance.

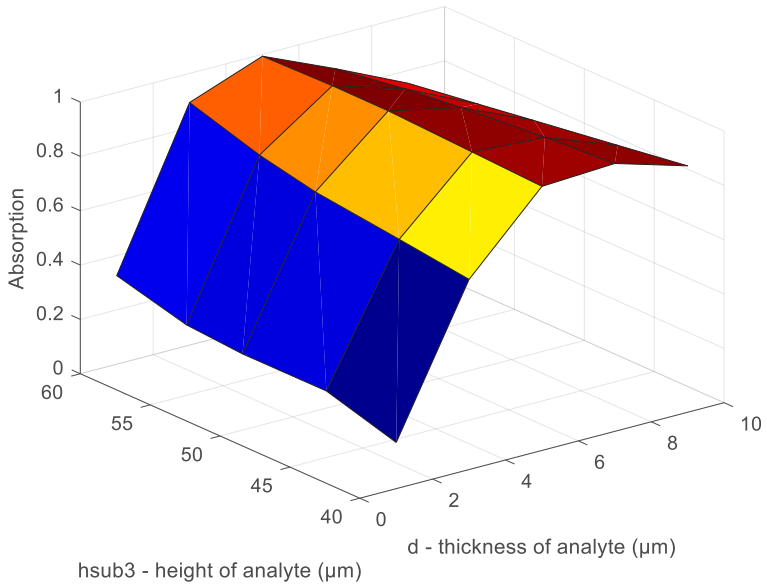

Fig. 10. Absorption graph with the change of radius and Height of analyte.

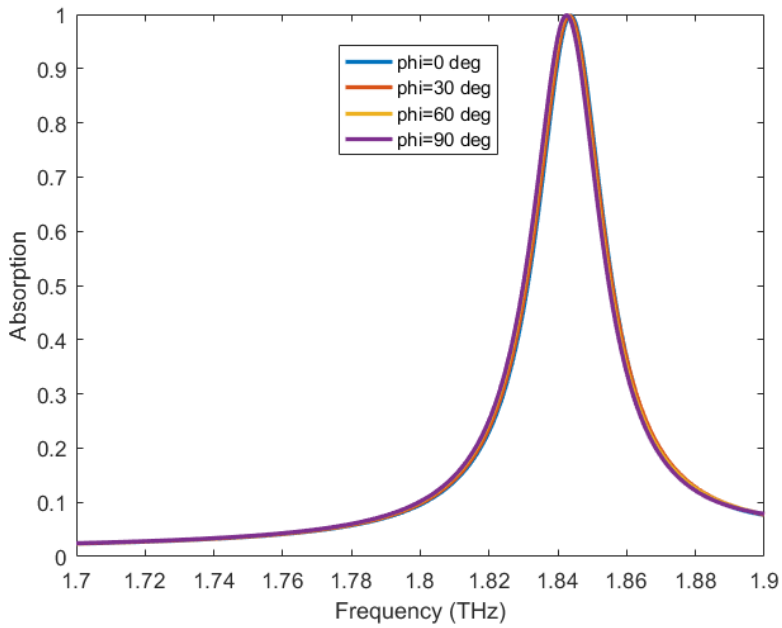

Fig. 11. Absorption of the sensor for different polarization angles of the incident incoming wave.

Table 2. Comparison between the performance of the work

Reference	Range of refractive index	*S* (GHz/RIU)	*Q-factor*	*FoM*
[10]	1-1.4	-	5.5	0.4
[6]	1-2.5	96.2	-	7.8
[11]	1.333-1.464	23.08	-	-
[12]	1-1.8	834	40.1	11.75
[13]	-	187	32.167	6.015
[5]	1-2	126	44.17	10.5
This work	1-2	166-672	69.1-116.2	10.2-29.7

Furthermore, Fig. 12(a), Fig. 12(b), Fig. 12(c), Fig. 12(d) and Fig. 12(e) are attained for 0, 45°, 90°, 100° and 135°, respectively. It should be noted that the maximum of the field inside the structure is about 2dB less than the amplitude of the imping plane wave.

4- Conclusion

In this paper, a metamaterial absorber has been introduced which is comprised of a cylindrical pipe cavity engraved in the upper layer of gold – topas – gold substrate. The sensing performance improvement of the structure is realized by adding a cylinder of InSb coaxially with the cavity. In the proposed structure, the excited SPPs on the surface of InSb propagate downward toward the cavity and through it. Based on the dimensions of the InSb cylinder, “High absorption” and “High-quality factor” sensing performance is defined and analyzed. It is shown that “high absorption” sensing performance is characterized by a relatively 100% absorption for measurement of the refractive index in the range of [1-2]. In the same way, the higher quality factor and nearly 100% absorption are achieved for the refractive indices in the range of [1.5-2], while absorption decreases to 60% if $n=1$ in “High-quality factor” sensing performance. Nearly 100% absorption, a wide range of refractive index measurements, and superior sensing performance besides the simplicity of the structure made this structure a good candidate for medical and biological THz sensing applications.

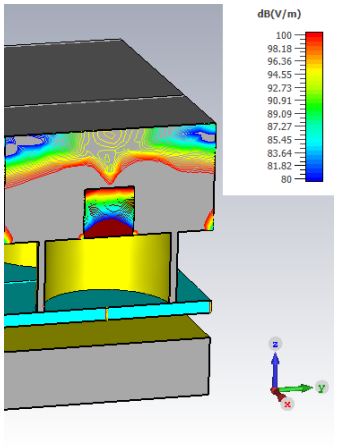

(a)

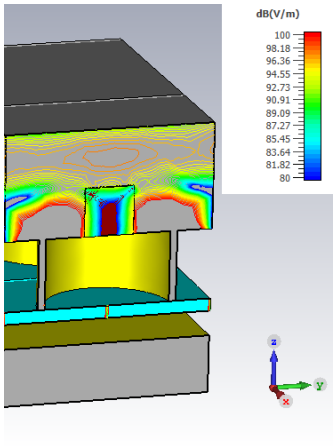

(b)

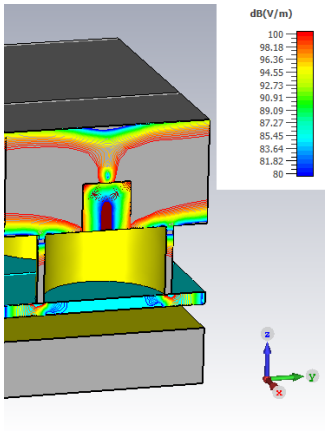

(c)

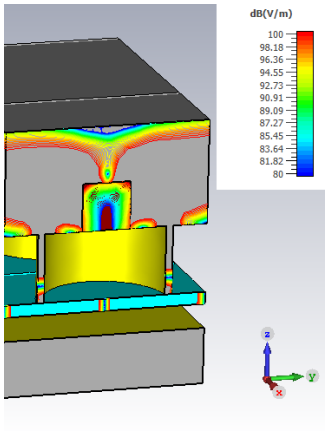

(d)

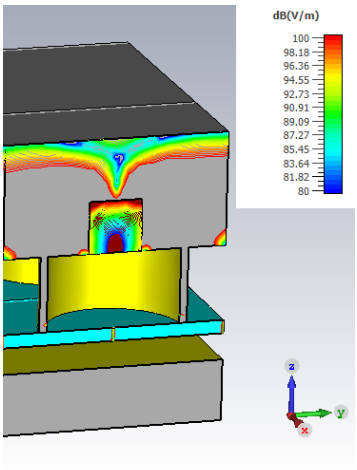

(d)

Fig. 12. Electric field propagation for different phases (a) 0º, (b) 45 º, (c) 90 º, (d) 100 º, and (e) 135 º.

References

[1] X. Chen and W. Fan, "Ultrasensitive terahertz metamaterial sensor based on spoof surface plasmon," Scientific Reports, vol. 7, no. 1, p. 2092, 2017/05/18 2017, doi: 10.1038/s41598-017-01781-6.

[2] A. S. Saadeldin, M. F. O. Hameed, E. M. A. Elkaramany, and S. S. A. Obayya, "Highly Sensitive Terahertz Metamaterial Sensor," IEEE Sensors Journal, vol. 19, no. 18, pp. 7993-7999, 2019, doi: 10.1109/JSEN.2019.2918214.

[3] F. Chen, Y. Cheng, and H. Luo, "Temperature Tunable Narrow-Band Terahertz Metasurface Absorber Based on InSb Micro-Cylinder Arrays for Enhanced Sensing Application," IEEE Access, vol. 8, pp. 82981-82988, 2020, doi: 10.1109/ACCESS.2020.2991331.

[4] M. Askari, "A near infrared plasmonic perfect absorber as a sensor for hemoglobin concentration detection," Optical and Quantum Electronics, vol. 53, no. 2, p. 67, 2021/01/22 2021, doi: 10.1007/s11082-020-02703-z.

[5] Z. Xiong et al., "Terahertz Sensor With Resonance Enhancement Based on Square Split-Ring Resonators," IEEE Access, vol. 9, pp. 59211-59221, 2021, doi: 10.1109/ACCESS.2021.3073043.

[6] W. Pan, Y. Yan, Y. Ma, and D. Shen, "A terahertz metamaterial based on electromagnetically induced transparency effect and its sensing performance," Optics Communications, vol. 431, pp. 115-119, 2019/01/15/ 2019, doi: https://doi.org/10.1016/j.optcom.2018.09.014.

[7] S. Banerjee, U. Nath, P. Dutta, A. V. Jha, B. Appasani, and N. Bizon, "A Theoretical Terahertz Metamaterial Absorber Structure with a High Quality Factor Using Two Circular Ring Resonators for Biomedical Sensing," Inventions, vol. 6, no. 4, doi: 10.3390/inventions6040078.

[8] M. S. Islam et al., "Broadband Characterization of Glass and Polymer Materials Using THz-TDS," in 2019 44th International Conference on Infrared, Millimeter, and Terahertz Waves (IRMMW-THz), 1-6 Sept. 2019 2019, pp. 1-2, doi: 10.1109/IRMMW-THz.2019.8874013.

[9] A. Mohanty, O. P. Acharya, B. Appasani, S. K. Mohapatra, and M. S. Khan, "Design of a Novel Terahertz Metamaterial Absorber for Sensing Applications," IEEE Sensors Journal, vol. 21, no. 20, pp. 22688-22694, 2021, doi: 10.1109/JSEN.2021.3109158.

HOW TO CITE THIS ARTICLE

S. Zamani Noughabi, A. S. Nooramin, M. Soleimani, Proposing a THz refractive index sensor based on the excitation of SPPs with an InSb cylinder, AUT J. Elec. Eng., 55(2) (2023) 133-144.

DOI: 10.22060/eej.2023.21972.5501